AD-A122 835 CONSIDERATIONS FOR THE DESIGN OF GROUND CLUTTER CANCELERS FOR WEATHER RAD..(U) NATIONAL OCEANIC AND ATMOSPHERIC ADMINISTRATION NORMAN OK NAT.. 1/1

UNCLASSIFIED D S ZRNIC' ET AL. JAN 82 DOT/FAA/RD-82/68 F/G 17/9 NL

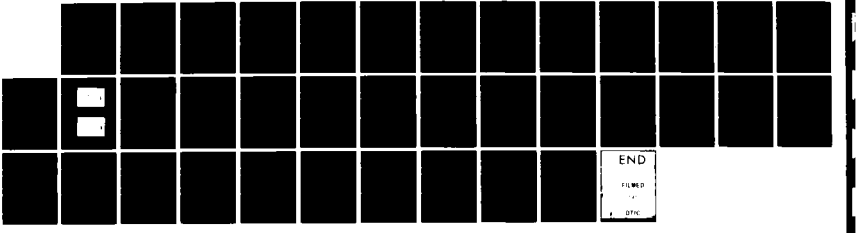

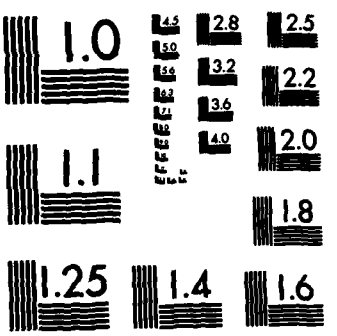

(13)

DOT/FAA/RD-82/68

Systems Research &
Development Service
Washington, D.C. 20590

Considerations for the Design of Ground Clutter Cancelers for Weather Radar

Dusan S. Zrnic'
Said Hamidi
Allen Zahrai

January 1982

Final Report

U.S. Department of Transportation
Federal Aviation Administration

NOTICE

This document is disseminated under the sponsorship of the Department of Transportation in the interest of information exchange. The United States Government assumes no liability for its contents or use thereof.

Technical Report Documentation Page

1. Report No.	2. Government Accession No.	3. Recipient's Catalog No.
DOT/FAA/RD-82/68	AD-A122 835	

4. Title and Subtitle	5. Report Date
CONSIDERATIONS FOR THE DESIGN OF GROUND CLUTTER CANCELERS FOR WEATHER RADAR	January 1982
	6. Performing Organization Code
7. Author(s)	8. Performing Organization Report No.
Dusan S. Zrnic', Said Hamidi and Allen Zahrai	
9. Performing Organization Name and Address	10. Work Unit No. (TRAIS)
National Severe Storms Laboratory 1313 Halley Circle Norman, OK 73069	11. Contract or Grant No. DTFA01-80-Y-10524
12. Sponsoring Agency Name and Address	13. Type of Report and Period Covered
Department of Transportation Federal Aviation Administration Systems Research and Development Service Washington, D.C. 20590	Final Report February 81 - January 82
	14. Sponsoring Agency Code ARD-230

15. Supplementary Notes

Prepared under FAA Interagency Agreement No. DOT-DTFA01-80-Y-10524, managed by the Surveillance Systems Branch, ARD-230.

16. Abstract

Effects of the ground clutter ring in the second trip area for velocity estimation are investigated. Besides unfavorable effects on weather signal due to range square advantage, the clutter poses a new problem when interlaced samples for assigning correct ranges to velocity estimates are used. The problem arises because signals that generate reflectivity estimates for power comparisons cannot be filtered in the same manner as signals from which velocity estimates are generated. Therefore, comparison of powers in the reflectivity and velocity channels is required. Performance of a third order recursive elliptic filter is analyzed. The filter operates best in steady state, but it can also be made to operate in transient by properly initializing its memory elements. Performance on 8 simulated time samples shows that about 10 dB of clutter to signal margin is lost for power and 20 dB for mean velocity estimation; with such a small number of samples, the width estimate is useless. In order for spectrum width biases to be less than 1 $m \cdot s^{-1}$, a longer train of pulses must be employed on an initialized filter and several of the leading pulses must be used exclusively to further reduce the transients. These problems do not arise when canceling is done on an uninterrupted pulse train. Examination of hardware for implementing the recursive filter demonstrates that two identical cancelers, one for the inphase, the other for the quadrature signal are needed. The device consists of an arithmetic and logic unit assisted by four multipliers; throughput rate is faster than 1 μs.

17. Key Words	18. Distribution Statement
Ground clutter canceler Doppler weather radar	Document is avilable to the U.S. public through the National Technical Information Service, Springfield, Virginia 22161

19. Security Classif. (of this report)	20. Security Classif. (of this page)	21. No. of Pages	22. Price
Unclassified	Unclassified	27	

Form DOT F 1700.7 (8-72) Reproduction of completed page authorized

METRIC CONVERSION FACTORS

Approximate Conversions to Metric Measures

Symbol	When You Know	Multiply by	To Find	Symbol
		LENGTH		
in	inches	*2.5	centimeters	cm
ft	feet	30	centimeters	cm
yd	yards	0.9	meters	m
mi	miles	1.6	kilometers	km
		AREA		
in^2	square inches	6.5	square centimeters	cm^2
ft^2	square feet	0.09	square meters	m^2
yd^2	square yards	0.8	square meters	m^2
mi^2	square miles	2.6	square kilometers	km^2
	acres	0.4	hectares	ha
		MASS (weight)		
oz	ounces	28	grams	g
lb	pounds	0.45	kilograms	kg
	short tons (2000 lb)	0.9	tonnes	t
		VOLUME		
tsp	teaspoons	5	milliliters	ml
Tbsp	tablespoons	15	milliliters	ml
fl oz	fluid ounces	30	milliliters	ml
c	cups	0.24	liters	l
pt	pints	0.47	liters	l
qt	quarts	0.96	liters	l
gal	gallons	3.8	liters	l
ft^3	cubic feet	0.03	cubic meters	m^3
yd^3	cubic yards	0.76	cubic meters	m^3
		TEMPERATURE (exact)		
°F	Fahrenheit temperature	5/9 (after subtracting 32)	Celsius temperature	°C

*1 in = 2.54 (exactly). For other exact conversions and more detailed tables, see NBS Misc. Publ. 286, Units of Weights and Measures, Price $2.25, SD Catalog No. C13.10:286.

Approximate Conversions from Metric Measures

Symbol	When You Know	Multiply by	To Find	Symbol
		LENGTH		
mm	millimeters	0.04	inches	in
cm	centimeters	0.4	inches	in
m	meters	3.3	feet	ft
m	meters	1.1	yards	yd
km	kilometers	0.6	miles	mi
		AREA		
cm^2	square centimeters	0.16	square inches	in^2
m^2	square meters	1.2	square yards	yd^2
km^2	square kilometers	0.4	square miles	mi^2
ha	hectares (10,000 m^2)	2.5	acres	
		MASS (weight)		
g	grams	0.035	ounces	oz
kg	kilograms	2.2	pounds	lb
t	tonnes (1000 kg)	1.1	short tons	
		VOLUME		
ml	milliliters	0.03	fluid ounces	fl oz
l	liters	2.1	pints	pt
l	liters	1.06	quarts	qt
l	liters	0.26	gallons	gal
m^3	cubic meters	35	cubic feet	ft^3
m^3	cubic meters	1.3	cubic yards	yd^3
		TEMPERATURE (exact)		
°C	Celsius temperature	9/5 (then add 32)	Fahrenheit temperature	°F

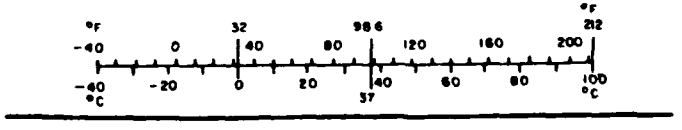

TABLE OF CONTENTS

List of Figures

Figure 15. Estimated mean signal spectrum width versus true width for simulated time series data. Thirty-two samples were filtered through the initialized filter but only the last sixteen were applied to the pulse pair processor. Clutter widths are 0.2 $m \cdot s^{-1}$ (upper graphs) and 0.4 $m \cdot s^{-1}$ (lower graphs). The mean signal velocities from left to right are 2, 8, and 24 $m \cdot s^{-1}$.

Figure 16. Frequency (velocity) response of a narrow notch filter. Solid line is for ideal coefficients and dashed line is with a 10-bit representation.

Figure 17. Frequency response of the filter on Fig. 16 except a 12-bit representation is used.

Figure 18. Block diagram of a ground clutter canceler. Coefficients are programmable and the filter can be of order up to three.

LIST OF TABLES

LIST OF ACRONYMS, ABBREVIATIONS, AND SYMBOLS

C/S or GC/SIG	Clutter to signal ratio (dB)
FIR	Finite impulse response filter
IIR	Infinite impulse response filter
L	Filter rejection (dB)
P_1	Power in the first trip
P_2	Power in the second trip
P_c	Clutter power
P_r	Clutter residue power

Powers in the reflectivity channel are primed and in the velocity channel are not.

PRT	Pulse repetition time
r_a	Unambiguous range
r_c	Extent of ground clutter in range
v	Mean velocity of weather signal
v_p	Passband cutoff velocity
v_s	Stopband cutoff velocity
σ_c or CLWD	Clutter spectrum width
σ_v or SIGWD	Doppler spectrum width of weather signal

The symbol ^ over a variable denotes an estimate.

CONSIDERATIONS FOR THE DESIGN OF GROUND CLUTTER CANCELERS OF WEATHER RADAR

Dusan S. Zrnic', Said Hamidi, and Allen Zahrai

1. Introduction

This final report relies heavily on the preceding interim report and is, in fact, its continuation and update. There is very little repetition and we often reference sections and equations from the interim report. Four main topics not covered in the interim report are dealt with herein.

The interim report studied the ground clutter properties at the Norman sites, and several canceling schemes were investigated. It was shown that clutter cross sections 40 to 50 dB below 1 m^2/m^2 are typical and that clutter spectrum widths range between 0.1 and 0.5 $m \cdot s^{-1}$ with the mean value of 0.25 $m \cdot s^{-1}$ at an antenna rotation rate of $10^0 s^{-1}$.

Design goals for the filter were 50 dB rejection in the stopband with a narrow variable notch width, a total annihilation at zero Doppler, and one dB ripple in the passband. Such goals can be achieved easily on contiguous pulse trains with either a recursive filter or a finite impulse response filter. However, if an interlaced pulse transmission scheme is utilized, canceling becomes difficult. The interlaced scheme is useful because it enables unambiguous measurement of reflectivity (at one pulse repetition frequency) and from it a correct assignment of ranges to velocity estimates that are obtained at another pulse repetition frequency. It was demonstrated that recursive filter with initialization does meet design specifications when the pulse train contains about 64 samples corresponding to a dwell time of about 50 ms. Under these conditions, similar performance can be obtained by properly weighting time series data before a Fourier transform is applied.

Section 2 treats problems that clutter causes in the second trip area (ring) for velocity estimation. These are increased area obscured by clutter and a disadvantage of second trip echo powers with respect to the first trip clutter power.

Assignment of correct ranges to velocity estimates when different clutter filters are used in the reflectivity and velocity channels is treated in Section 3.

The thrust of this report is in the investigation of the recursive filter performance when a small number of pulses (eight) is passed through the filter. This is treated in Section 4. As in the interim report, the quality of filters performance is judged from the biases in the mean velocity and spectrum width

estimates obtained by a pulse pair processing algorithm behind the filter.

Finally, in Section 5 are presented some engineering design considerations for the recursive filter. This filter is presently being built in support of the NEXRAD requirements.

2. Effects of Ground Clutter Ring in the Second Trip Area

Ground clutter ring in the second trip area impedes velocity estimation because clutter there competes with weather signals that have a range squared disadvantage. Furthermore, the area covered by clutter is larger in the second trip than in the first. We illustrate this by way of an example on NSSL's Norman Doppler radar. The first trip area at three elevation angles for which clutter is larger than -10 dBZ is shown on the histograms (Figure 1) and in Table 1. Also listed in the table is the extent of clutter in range r_c. The area A_2 covered in the second trip (for an unambiguous range r_a = 115 km) is

$$A_2 = \pi r_c^2 + 2\pi r_c r_a \qquad (1)$$

which translates to over 10 times as much as in the first trip (see Table 1)! The percentage of the obscured first trip area is only between 2.4 and 4.7 percent, but the percentage of the second trip area ($3\, r_a^2 \pi$) that is obscured ranges from 11 to 16 percent. Figures 2 and 3 illustrate this effect for the elevation angle of 0.8°.

Range advantage of close targets for an unambiguous range of r_a = 115 km is drawn on Figure 4. In order to have accurate mean velocity estimates (bias less than 1 $m \cdot s^{-1}$) from the pulse pair algorithm, the weather signal must be 10 dB larger than any spurious components including clutter (Zrnic' and Hamidi, 1981). Consequently, a patch of clutter at a range 10 to 15 km with an equivalent reflectivity factor of 10 dBZ competes with weather signals up to 40 dBZ in strength when these are at 125 to 130 km.

3. Range De-Aliasing of Velocity Estimates when Clutter Filtering is Employed

We shall now point out some difficulties that are inherent to a dual sampling mode if one tries both to eliminate the clutter and to assign correct ranges to velocity estimates. To illustrate the problem, consider a simplified interlaced scheme that uses a pulse repetition time T_s for velocity estimation and $2T_s$ for reflectivity (Figure 5).

This scheme is conceptually identical to the one used on NSSL radars except for the $2T_s$ reflectivity PRT (NSSL radars use $4T_s$). However, by restricting ourselves to first and second trip echoes only, we avoid needless complications while

Table 1. Area and average range extent of clutter for the Norman site at three elevation angles.

Elevation (°)	Area in First Trip Where Clutter >-10 dBZ (km^2)	Average Range Exient of Clutter r_c (km)	% of First Trip Area Obscured	Area in Second Trip where C >-10 dBZ (km^2)	% of Second Trip Area Obscured
0	2000	25	4.7	20,000	16
0.4	1700	23	4	18,000	15
0.8	1000	18	2.4	14,000	11

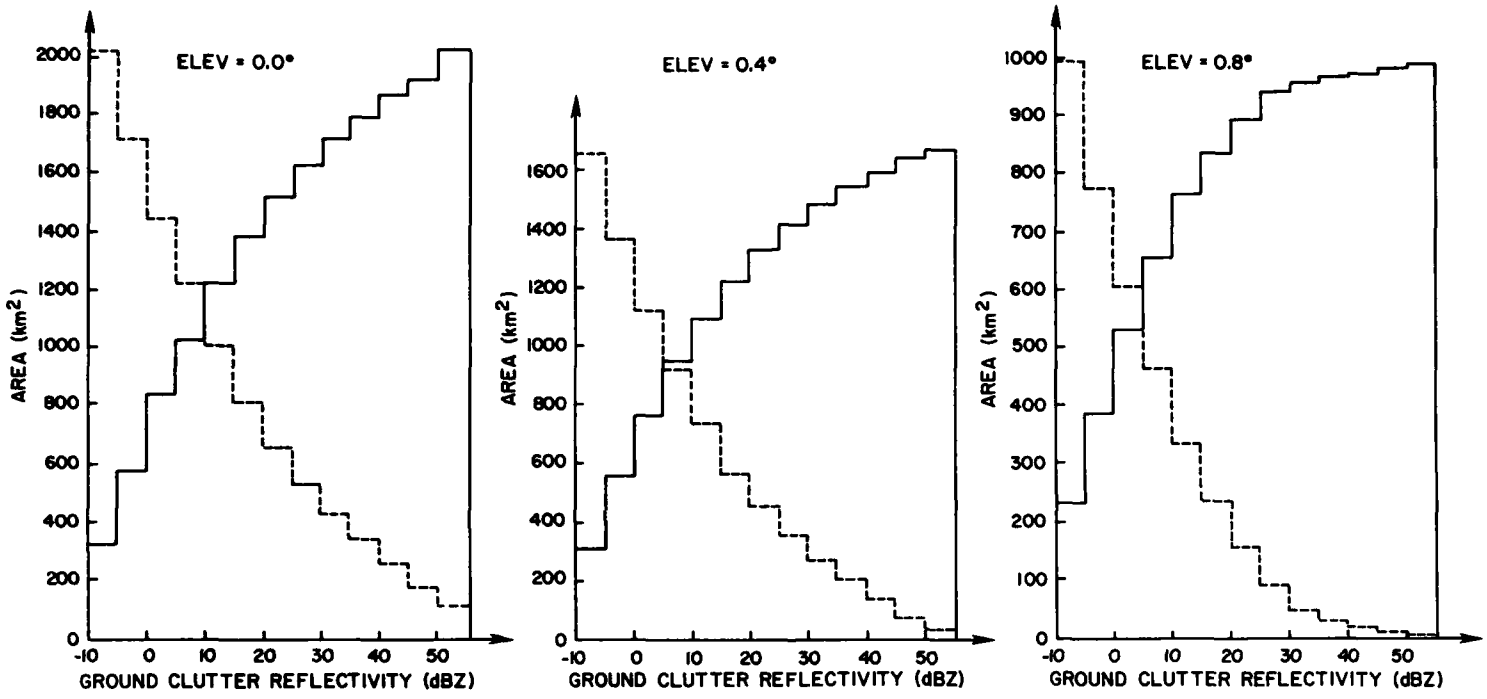

Figure 1. Cumulative areas of ground clutter for three elevation angles of the Norman site. The total with respect to which data are taken represents all returns larger than -10 dBZ. The last category contains values larger than 50 dBZ. During data collection, there were no noticeable echoes from clear air or insects. Dashed line signifies areas with clutter power equal or larger than the abscissa. Solid line is for powers less or equal to the abscissa

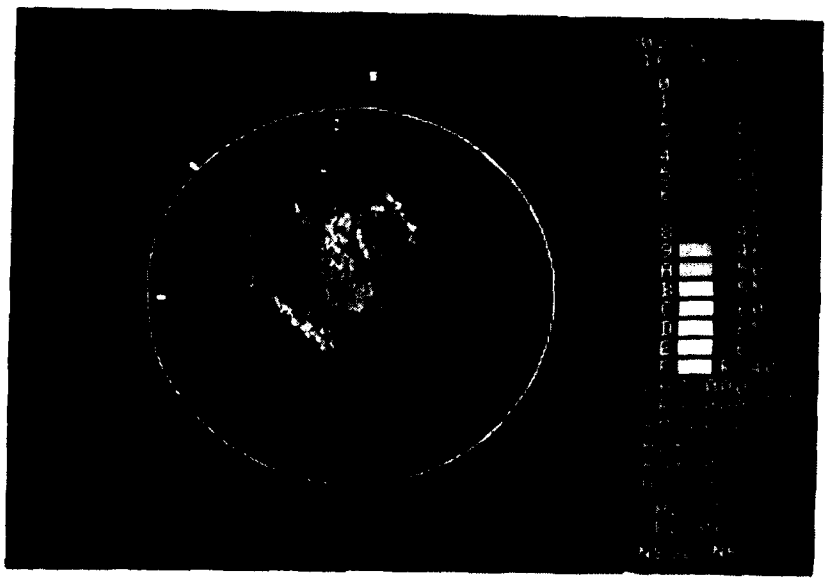

Figure 2. Ground clutter at 0.8° elevation, first trip.

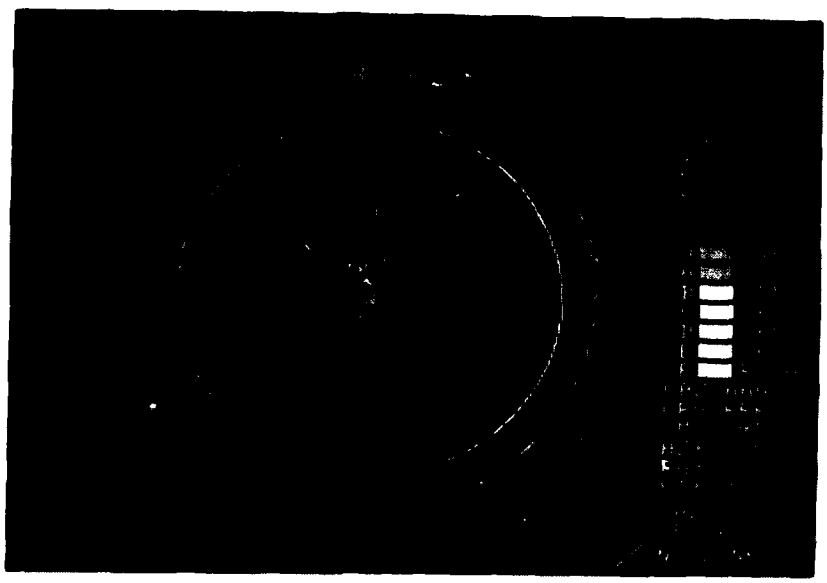

Figure 3. Ground clutter in both trips at 0.8° elevation.

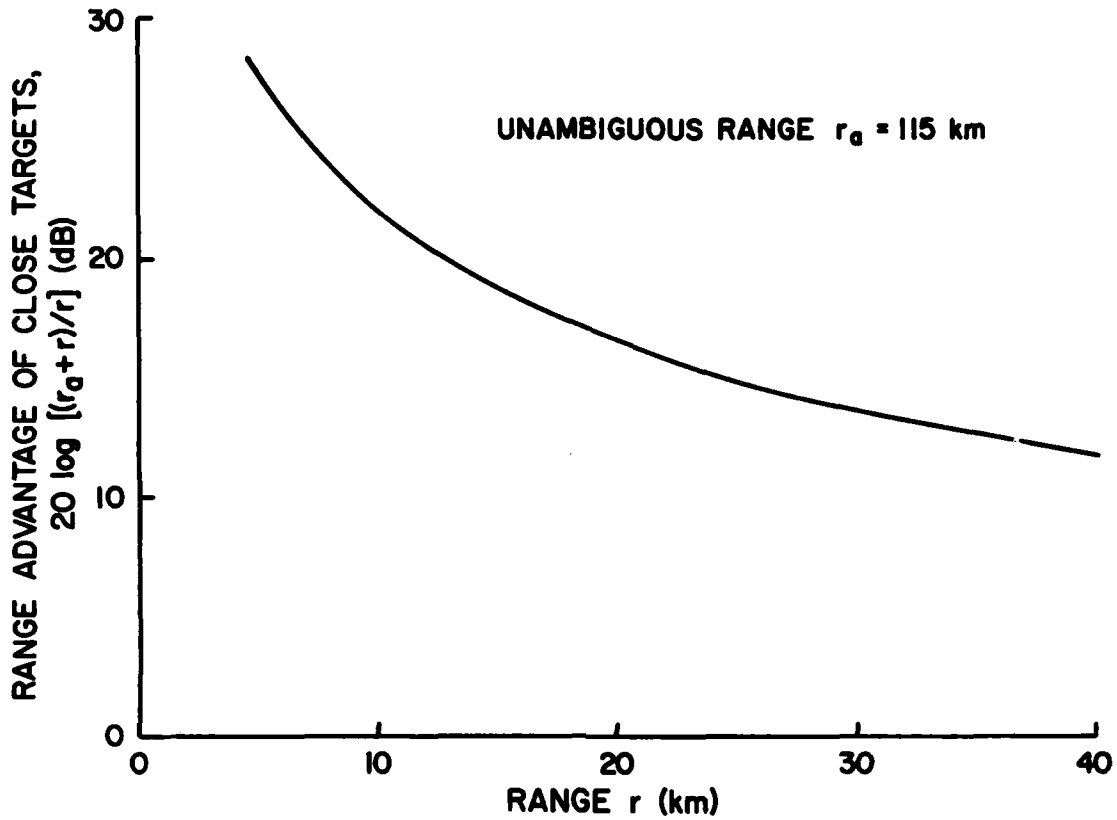

Figure 4. Range advantage of first trip weather echoes over second trip weather echoes.

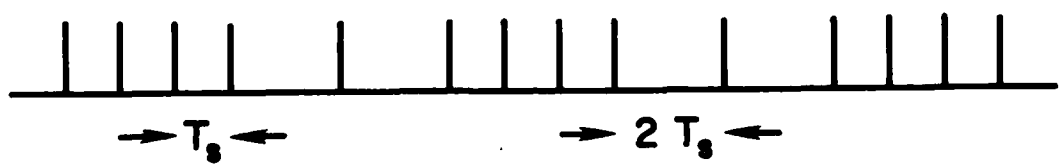

Figure 5. Interlaced pulse transmission scheme.

retaining essential aspects of the problem.

Figure 6 illustrates how the present range-unfolding algorithm works in presence of ground clutter and first and second trip storms (Hennington, 1981). The algorithm examines three possibilities by comparing powers in the reflectivity channel for each resolution volume: 1) the first trip power P_1 is larger than the second trip power P_2 by 10 dB. Then first trip velocities are unbiased, and any overlaid second trip echo is not usable. 2) $P_2 \geq 10\ P_1$; the second trip velocities are valid, and weakly scattering first trip targets are obscured. 3) The powers are within 10 dB from each other, and velocities cannot be assigned to targets in either trip. Radar equipped with phase diversity could recover part of this area in both trips. The recoverable area depends on the signal-to-noise degradation that one is able to tolerate. For instance, if the first and second trip signals have equal powers and one is made incoherent, the signal to "white noise" ratio over the Nyquist interval becomes 0 dB.

Introduction of a ground clutter canceler in a Doppler channel changes the situation because the powers now from the first trip clutter are different in the two channels. In principle, the optimum scheme is a dual frequency radar with identical clutter filters in the coherent reflectivity and velocity channels so that the power comparison algorithm would work. This is so because with two frequencies the dwell time for reflectivity estimation can be made long enough to insure satisfactory filtering. Thus, the shapes of filter notches and ripples in the passband can be made almost equal. But then a second coherent receiver is needed and possibly a log channel for AGC (if instantaneous AGC is not contemplated). Although the notch and ripple can be made equal, the two filters necessarily have different Nyquist velocities, with the one for reflectivity being smaller (by a factor of 2 for the example on Figure 5). Consequently, there may be powers from storms with velocities that have aliased into the notch of the filter in the reflectivity channel. These would be canceled while no similar canceling would occur in the velocity channel. In such cases, the algorithm based on power comparisons in the reflectivity channel would be erroneous.

In the remainder of this section we consider range assignment of velocity estimates when a single frequency radar is used in an interlaced mode. We assume that several batches of higher PRT pulses in the velocity channel are interlaced with short bursts, one or at most two pulses, in the reflectivity channel. A scheme with eight pulses for velocity (see section 4) and two for reflectivity is workable with a possibility of crude (difference) canceling in the reflectivity channel. In the sequel we imply that the reflectivity channel is used to set AGC

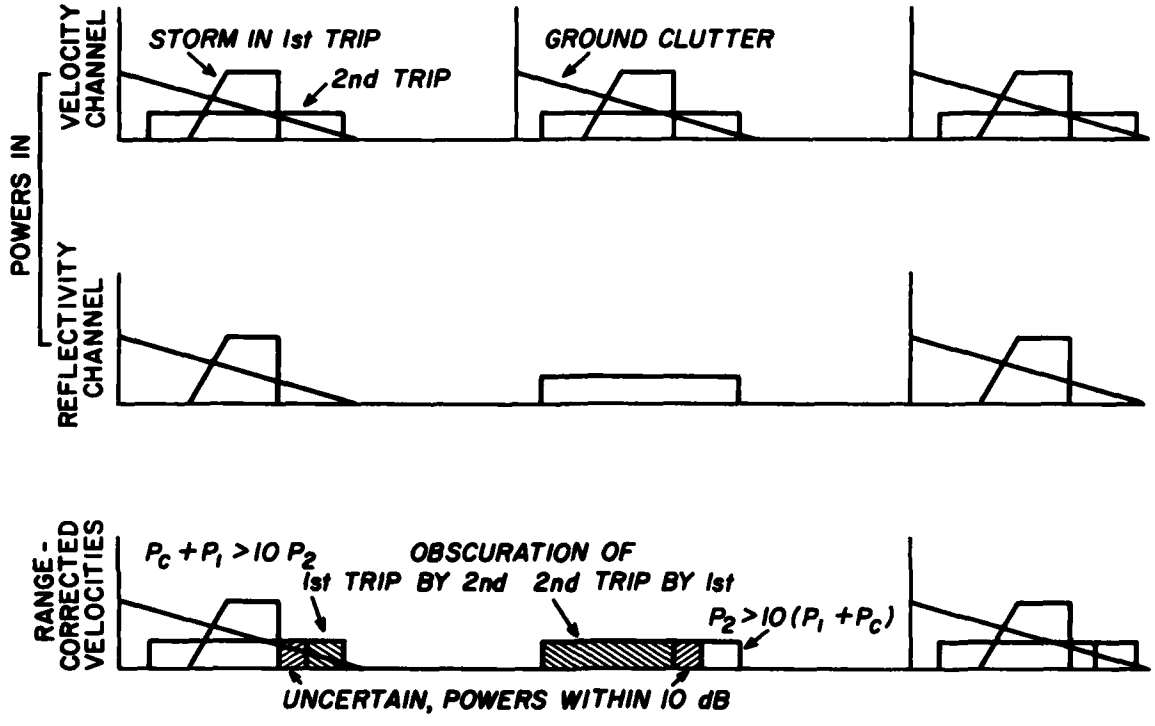

Figure 6. Illustration of obscuration in the velocity and reflectivity channels for the transmission scheme as on Figure 5.

and de-alias range overlaid velocities by comparing powers in the two channels. The reflectivity measurements should also be made from the velocity channel except at times when storms are overlaid. Even in the absence of second trip echoes, the powers in the two channels are not going to be exactly equal because they are not estimated from the same samples in the interlaced mode (this difference is statistical). Moreover, the quantization noise and slight nonlinearities between the transfer functions of the two channels cannot be perfectly accounted for (this difference is systematic). To make this distinction, the clutter and signal powers from the reflectivity channel are primed (Table 2). The input powers in the reflectivity channel are clutter and first trip echo $\hat{P}_{z1}=P'_c+P'_1$ or power P_{z2} which corresponds to the second trip echo for the velocity channel (Figure 7). In the velocity channel, powers in general are clutter from first and signals from both trips $\hat{P}_v=P_c+P_1+P_2$.

At the output of the clutter filter in the velocity channel, the clutter residue power is P_r and in the reflectivity channel clutter residue is P'_r.

Table 2 illustrates the powers when first and second trip targets are sampled in the reflectivity channel. Both trip targets are sampled simultaneously in the velocity channel.

Now it suffices to compare the power P'_2 in the reflectivity channel with the filtered power P_{vf} in the velocity channel. We assume that all the powers are sufficiently higher than the receiver noise. Thus range de-aliasing proceeds as follows:

1) If $P_{vf} > 10\,P'_2$, velocities are from first trip clutter residue and first trip echo. (Calculation of reflectivity should be from velocity channel.)

2) If $2P'_2 < P_{vf} < 10P'_2$, recovery of velocities is not possible. (Reflectivities calculated from reflectivity channel.)

3) If $P_{vf} < 2P'_2$, velocities are from the second trip signal. (Reflectivities calculated from velocity channel.)

Note that in this interlaced mode, assignment of ranges to the first trip is very satisfying since errors of the order of 1 dB in P_{vf} and P'_2 do not significantly affect the comparison #1. Not so in the comparison #3. Ideally, one would want to have P_1 plus the clutter residue power P_r smaller by 10 dB from P_2. But because the filter gain in the passband varies by ±1 dB and because of previously mentioned uncertainties, comparison #3 is chosen. Therefore, when condition #3 is satisfied, there will be times when erroneous velocities are obtained because P_r+P_1 may not be smaller than 0.1 P_2. On the other hand, if the condition is

TABLE 2

Powers in the velocity and reflectivity channels for the transmission scheme as on Fig. 5.

First Trip Targets Sampled

	Before filter	After filter
Velocity	$\hat{P}_v = P_c + P_1 + P_2$	$\hat{P}_{vf} = P_r + P_{1f} + P_{2f}$
Reflectivity	$\hat{P}_{z1} = P'_c + P'_1$	$\hat{P}_{z1f} = P'_r + P'_{1f}$

Second Trip Targets Sampled

	Before filter	After filter
Velocity	$\hat{P}_v = P_c + P_1 + P_2$	$\hat{P}_{vf} = P_r + P_{1f} + P_{2f}$
Reflectivity	$\hat{P}_{z2} = P'_2$	$\hat{P}_{z2f} = P'_{2f}$

$P_{1f} \approx P_1$ and $P_{2f} \approx P_2$ for targets far removed from zero velocity; filter ripple is small; and gain is near unity.

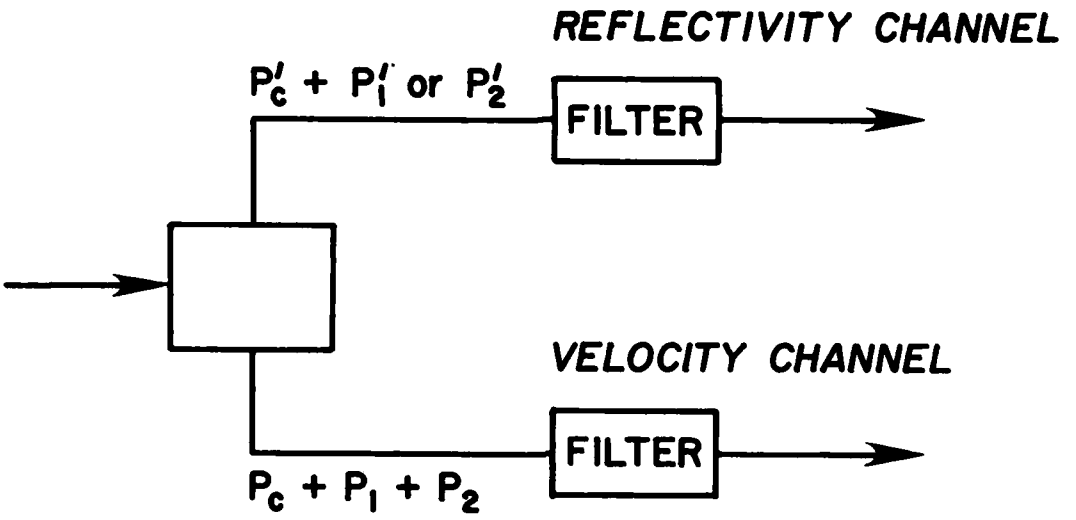

Figure 7. Block diagram of the reflectivity and velocity channels with ground clutter filters.

changed to $P_f < 1.1\ P_2'$, more data will be lost, and still some may be erroneous due to the statistical and systematic uncertainties. A phase diversity radar would help in this instance because biases (due to larger values of P_r+P_1 allowed by #3) would be eliminated at the expense of increased standard errors of estimates.

Our discussion carries to other choices of the two PRT's. For instance, if reflectivity is estimated with a PRT of $3T_s$, one needs to make a comparison in the reflectivity channel of powers in the second P_2' and third P_3' ambiguous range ring for velocity estimation. So wherever $P_2' \geq 10\ P_3'$, assume significant power is in second trip, and compare $P_2'+P_3'$ with P_{vf} as in #1 to #3. Whenever $P_3' > 10\ P_2'$, assume significant power is in third trip, take $P_2'+P_3'$ and proceed with #1 to #3. If P_2' and P_3' are within 10 dB of each other, data in second and third trip are contaminated, take $P_2'+P_3'$ and compare as in #1 to #3.

Although recovery of the second trip storm velocities if overlaid by ground clutter and first trip storm echo is not satisfactory, the overall performance of the radar will be good. First, we must bear in mind that occurrence of triple overlay is rare. Second, when only ground clutter overlays the storm in the second trip, a good canceler (50 dB) will reduce clutter residue to a negligible value in most of the area so that comparison #3 will produce valid data.

An alternate method to assign velocities is by comparison of powers in the reflectivity channel after the filter. This is equivalent to the present scheme on NSSL radars (except that they don't yet have a clutter filter in the reflectivity channel). If such a comparison were made, the full benefit of the filter in the velocity channel would not be realized; a clutter filter in the reflectivity channel (when interlaced samples are used) would cancel less than the filter in the velocity channel because the number of samples for reflectivity measurements is several times smaller than for velocity measurements.

4. The Third Order Recursive Filter

For accurate mean velocity estimation (rms error $\leq 1\ m \cdot s^{-1}$) via the pulse pair processor, one needs a 10 dB ratio of signal to clutter residue and 15 dB ratio if spectrum width is estimated (Zrnic' and Hamidi, 1981). Thus, the canceler must reduce the residue to at least 10 dB below signal power. Therfore, a 50 dB canceler would allow moment estimation up to about 40 dB of clutter C to signal S power ratio.

We consider a 50 dB rejection in a stopband, a 1 dB ripple in the passband, and a transmission zero at DC, reasonable goals to achieve since a recursive filter with such characteristics has already been designed and fabricated by Raytheon

engineers (Groginsky and Glover, 1980). Incidentally, no more than 50 dB of cancellation is possible if an 8-bit A/D converter is used because when the clutter spans the full 8-bit range, its quantization noise is 50 dB below its average power.

In Table 3, we list a third order filter that we have analyzed, and on Figure 8 is the appropriate flow chart that defines the k coefficients. For illustration, the transfer characteristic of the filter is shown in Figure 9 where the stopband cutoff velocity v_s and passband cutoff velocity v_p are also defined.

The main disadvantage of the recursive elliptic filter is its transient response. Although the steady state frequency response of IIR (Infinite Impulse Response) filters may compare well with FIR (Finite Impulse Response) filters, infinite duration of their impulse response has limited use in radar application. At low elevation angles (0.5°) the clutter power is several orders of magnitude stronger than the signal power. Thus, when interlaced samples (batch) for velocity and reflectivity estimation are used (Doviak et al., 1979), the clutter appears as a step to the filter which produces severe ringing at the output and in effect overwhelms the signal. A similar condition occurs if the automatic gain control (AGC) changes the gain just before processing a block of pulses. To reduce this effect, either enough time must be allowed for the transients to settle before pulse pair processing is attempted or some other means of their suppression must be employed. Because settling time is tens of pulses, we consider the alternative which is initialization (Fletcher and Burlage, 1972). The purpose of initialization is to load the memory elements of the recursive filter with their anticipated steady state values. These values can be estimated from the first incoming pulse. When the ground clutter is a perfect D.C. line and no weather signal is present, the initialization will immediately bring the filter into steady state. However, the clutter has finite width and superposed on it is the weather signal which together degrade the initialization.

For the third order filter on Figure 8, the output of the first memory element, Z^{-1}, would be set to $A_1(1-K_4)$ where A_1 is the digital value of the first sample. The outputs of the other two elements must be set to 0. With this, the output after the first time sample, A_1, is 0 and after the second one, A_2, it is A_2-A_1. Thus, the filter immediately acts as a delay line canceler so that a large D.C. value does not get through.

The expected clutter attenuation for an initialized filter is 25 dB more (in transient) than for the noninitialized filter (Figure 10). Attenuations were computed from the expected power at the filter's output for a given recursion, Increase in spectrum width reduces the attenuation because more skirts of the

Table 3. Coefficients for the high pass elliptic filter (PRT=781 μs, λ = 10 cm).

f_p	v_p	f_s	v_s	k_1	k_2	k_3	k_4
Hz	(m/s)	Hz	(m/s)				
60	2.9	17.0	0.8	1.995322175	1.802510637	0.871228116	0.577292360

clutter spectrum spill into the passband. It is noteworthy that the transient for the initialized filter lasts about 50 recursions but for the noninitialized it is over 100. Moreover, the initialized filter can be quite effective even in transient because the attenuation is considerable. At the first recursion the noninitialized filter does not attenuate clutter due to a direct path between input and output (Figure 8). This is not so for the initialized filter where the output starts at a second recursion.

In the interim report (Zrnic and Hamidi, 1981), the following equation relating the clutter spectrum width σ_c, the passband velocity v_p and the frequency domain rejection L (dB) was derived:

$$v_p = \sigma_c \frac{L}{5 \log e} . \tag{2}$$

For a 50 dB rejection, this becomes

$$v_p \geq 4.8 \sigma_c \tag{3}$$

Using calculations that lead to Figure 10, we have obtained another relationship between σ_c and v_p for a fixed integrated attenuation. The attenuation in steady state decreases with the increase in clutter spectrum width (Figure 11), and we note 50 dB or more attenuation is for widths

$$\sigma_c < 0.44 v_s \tag{4}$$

For this type of filter $v_p \approx 3.6 v_s$ and in order to keep the total residual power below 50 dB we find

$$v_p > 8.2 \sigma_c \tag{5}$$

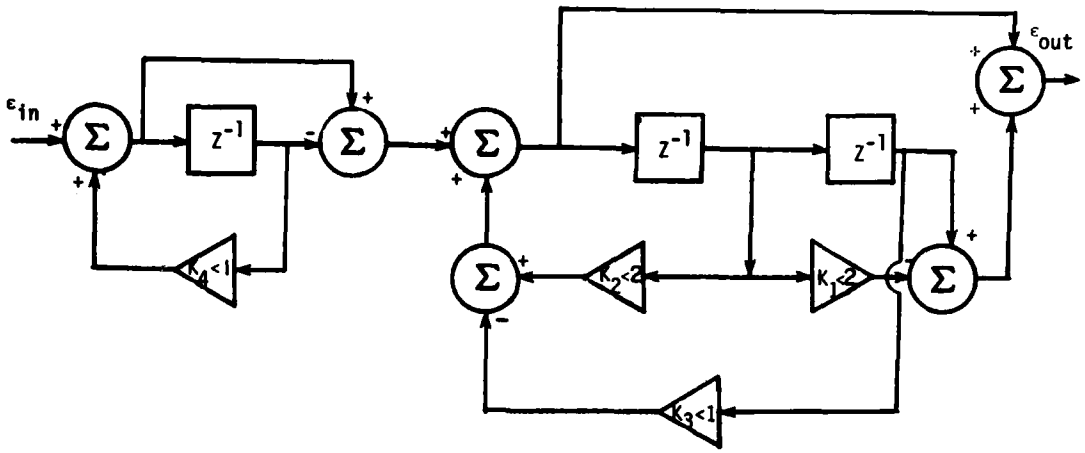

Figure 8. Block diagram of the third order high pass elliptic filter.

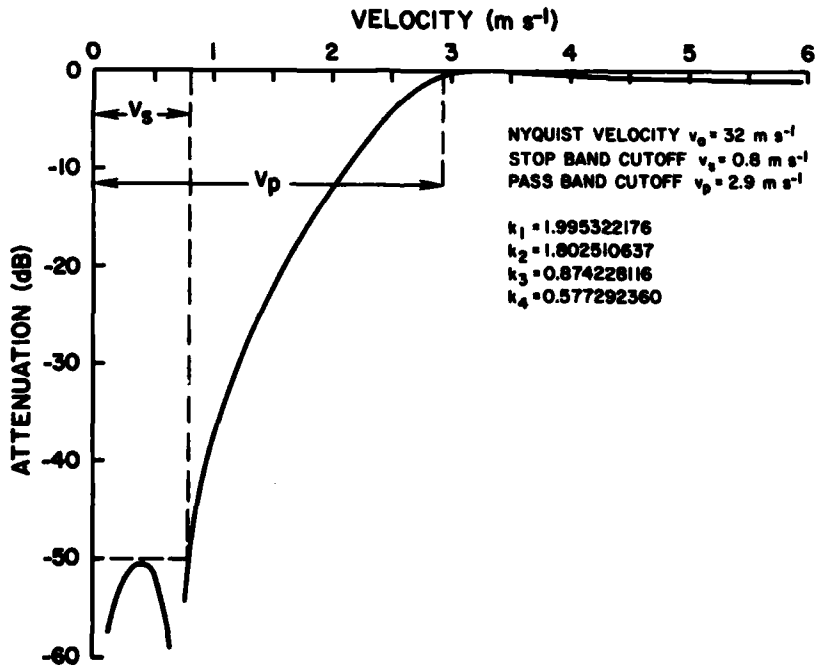

Figure 9. Frequency (Doppler velocity) response characteristic of the recursive filter. The Nyquist interval is 64 $m \cdot s^{-1}$.

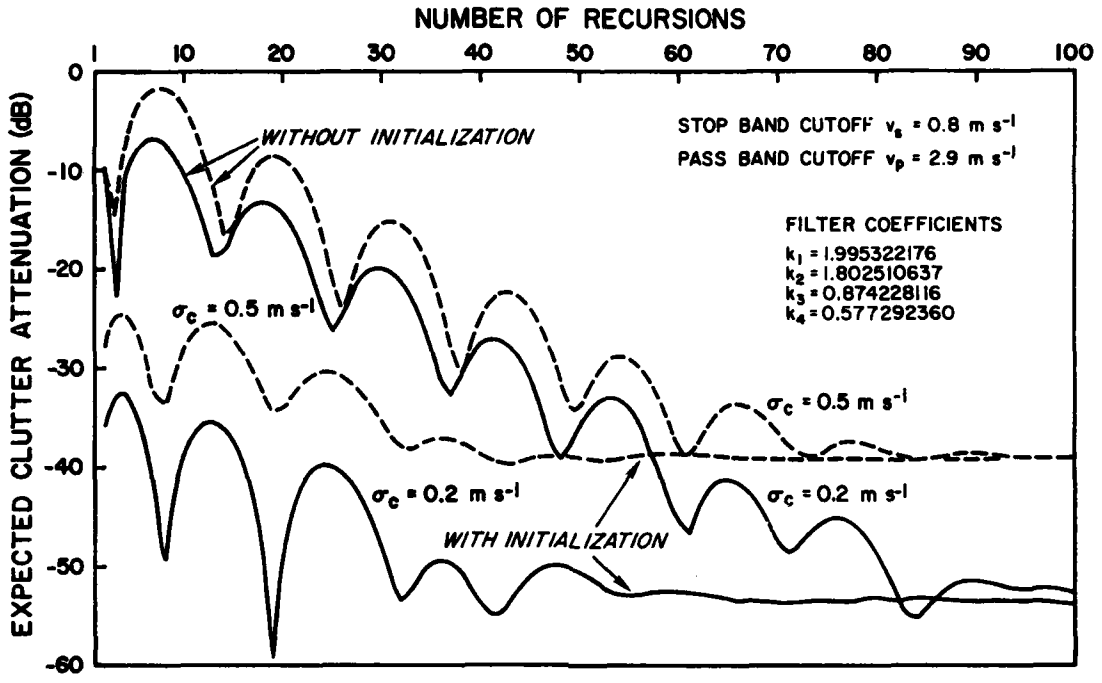

Figure 10. Expected attenuation after a clutter step is applied to the filter. Two clutter spectrum widths, $\sigma_c = 0.2\ m \cdot s^{-1}$ and $\sigma_c = 0.5\ m \cdot s^{-1}$ are considered for both the initialized and noninitialized filter.

The recursive filter operates on each component of the complex digital video samples before the pulse pair processor (Figure 12). In addition to the mean velocity $\hat{v}$ and spectrum width $\hat{\sigma}_v$ estimates, the processor provides an estimate of echo power $\hat{P}$. Power is computed from a uniform average of the square of time sample magnitudes. Mean velocity is from the argument of the autocovariance at lag one and the spectrum width from the logarithm of the correlation coefficient at lag one. For short, we call all three pulse pair processing.

To illustrate the performance of the initialized tandem filter-pulse pair processor, simulations on synthetic time series data and on some real data were conducted. Roundoff effects on coefficients and finite word lengths of data were not considered. Groginsky and Glover (1980) show that coefficients with 12- to

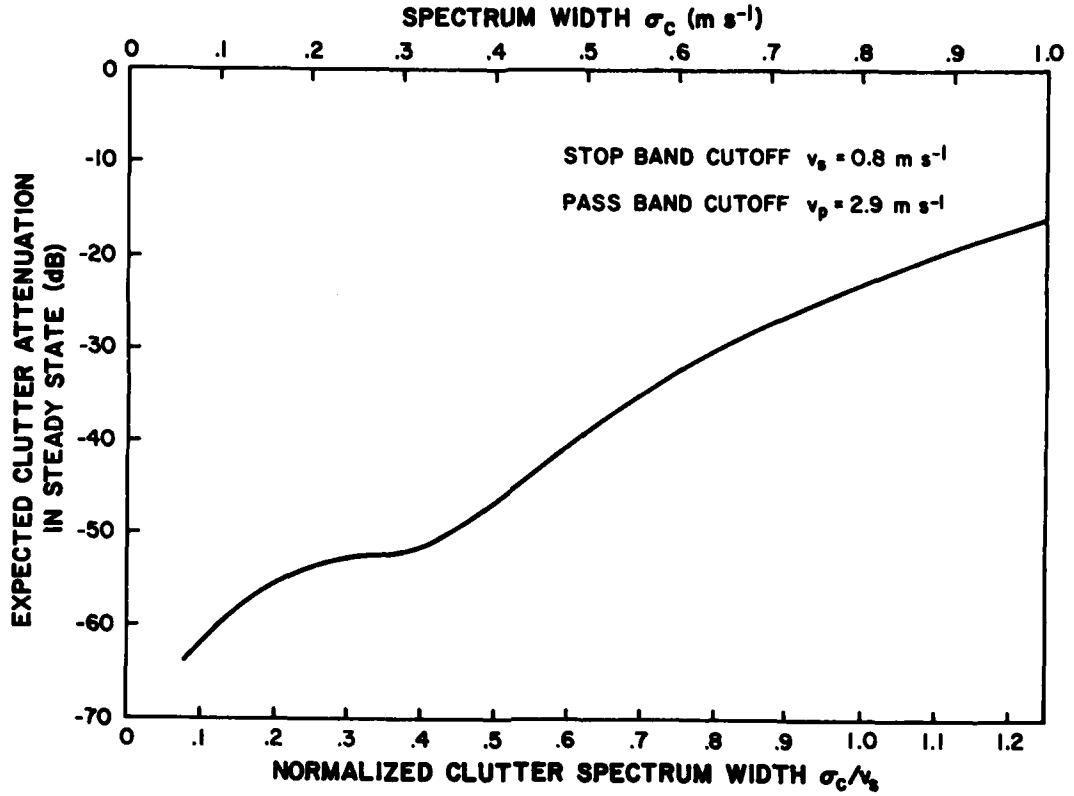

Figure 11. Expected clutter attenuation for a filter in steady state.

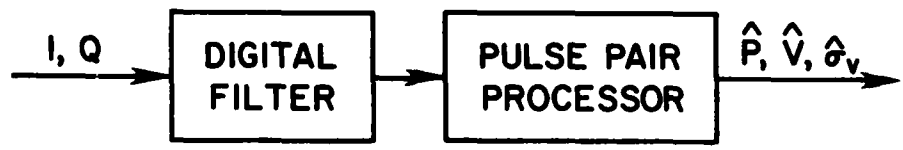

Figure 12. Block diagram of data flow. I and Q are the digitized video signals that must be filtered prior to pulse pair processing.

16-bit word lengths (depending on radar PRT) do not degrade the filter performance (see section 5).

Digital computer simulation of the block diagram on Figure 12 tested the quality of the output after filtering. The input time series data were synthesized such that they contained a clutter and weather signal of Gaussian spectral shapes and had Gaussian statistics (see Zrnic', 1975, for details). Unambiguous velocity, v_a, was set to 32 $m \cdot s^{-1}$.

In the results that follow, eight complex time samples were passed through the filter and estimates $\hat{P}$, $\hat{v}$, and $\hat{\sigma}_v$ were computed. We consider eight contiguous pulses to be close to a lower limit as far as standard errors of estimates is concerned. These errors are less than about 3 $m \cdot s^{-1}$ in both spectrum width and velocity if widths are less than 8 $m \cdot s^{-1}$ (Zrnic', 1979b). The actual number of contiguous pulse pairs out of eight pulses becomes six since the first pulse is lost in the process of initialization.

Even if 3 $m \cdot s^{-1}$ errors are not tolerable, groups of eight pulses might be used in an interlaced pulse scheme to estimate velocity and spectrum width. The reflectivity is obtained from a separate pulse with a clearing period to achieve large unambiguous range. Comparison of powers in the reflectivity channel enables one to assign correct ranges to the velocity estimates that have a small unambiguous range (Doviak et al., 1979). This technique requires that coherent and incoherent estimates are from echoes that originate in overlapping resolution volumes; a small number of contiguous samples for velocity and spectrum width estimates insures enough overlap. Hence, our choice of eight pulses is justified on one more ground.

Mean values of the estimates $\hat{P}$, $\hat{v}$, and $\hat{\sigma}_v$ can serve to quantify the comparison between a noninitialized and initilized filter because these estimates are the final product of interest. Blocks of 8 time samples were applied repeatedly 100 times to the recursive filter and that many estimates of power, velocity and spectrum width were obtained. The estimates were then averaged to generate the mean values. Throughout this simulation three clutter widths, σ_c = 0.2, 0.4, and 0.6 $m \cdot s^{-1}$ were examined because the first one, 0.2 $m \cdot s^{-1}$, is much narrower than the filter notch; the second, 0.4 $m \cdot s^{-1}$, is only slightly larger (by 0.05 $m \cdot s^{-1}$) than the value allowed by inequality (3); and 0.6 $m \cdot s^{-1}$ satisfies the inequality in (5). Also, the percentage of occurrences of clutter widths below 0.6 $m \cdot s^{-1}$ (for the Norman radar) is about constant, but drops rapidly after 0.6 $m \cdot s^{-1}$ if the antenna is rotating at 10°s (see Figures 1.9, 1.10, and 1.11 in Zrnic' and Hamidi, 1981).

Clutter-to-signal ratios of 10, 20, 30, and 40 dB for the initialized filter, and ratios of -10, 0, 10, and 20 dB for the noninitialized one were examined. As expected, power estimates from the initialized filter are less than one dB from their true values as long as C/S $\leq$ 30 dB and the mean velocity is larger than 8 $m \cdot s^{-1}$ (Figure 13). At a narrow signal spectrum width (e.g., 1 $m \cdot s^{-1}$), near zero velocity the filter removes quite a bit of power, but at a width of 8 $m \cdot s^{-1}$, at most 3 dB is lost. Clutter power must be reduced by about 20 dB in order to achieve comparable performance with a noninitialized filter.

Mean velocity estimates (Figure 14) also illustrate the improved performance of the initialized filter. The first sample was dropped and six pairs (out of seven possible) were used in order to have the same number for two filter conditions (i.e., initialized and noninitialized). Note that the initialized filter is effective up to 20 dB of clutter-to-signal ratio, which is 20 dB better than the noninitialized case. A slight positive bias at small velocities and weak clutter is due to loss of the portion of weather spectrum near the origin. Otherwise, strong clutter, 30 or more dB above signal, creates unacceptable bias. Thus, as far as mean velocity bias is concerned, this filter with a 50 dB notch when properly initialized acts like a 30 dB filter (which includes the 10 dB margin discussed in the beginning of this section). Without initialization, the effective attenuation is only 10 dB, which can be deduced from the fact that at C/S = 0 dB a good mean velocity estimate (bias about 1 $m \cdot s^{-1}$) is obtained. To achieve similar results without the filter, clutter power must be 10 dB below signal.

Spectrum width estimates had unacceptable bias that depends on clutter-to-signal ratio, mean velocity, and spectrum width. For instance, with mean velocity of 24 $m \cdot s^{-1}$ (i.e., 3/4 Nyquist velocity) and C/S = 10 dB, bias was larger than 3 $m \cdot s^{-1}$. Such large bias is due to the transients (damped sinusoid) of the second order section. These transients create symmetrical sidebands around zero velocity.

It is possible to reduce the disastrous effect of transient on spectrum width by having a longer train of pulses and ignoring several of those at the beginning. Figure 10 may guide the determination of the number of samples that should be allowed for transients to settle, in order to obtain good clutter canceling. For instance, if the first 16 filtered samples are dropped, the clutter with a spectrum width of 0.2 $m \cdot s^{-1}$ is attenuated by over 36 dB. The examples on Figure 15 was obtained when 32 pulses were passed through the initialized filter and the last sixteen are used for width calculation. Results are satisfactory (biases less

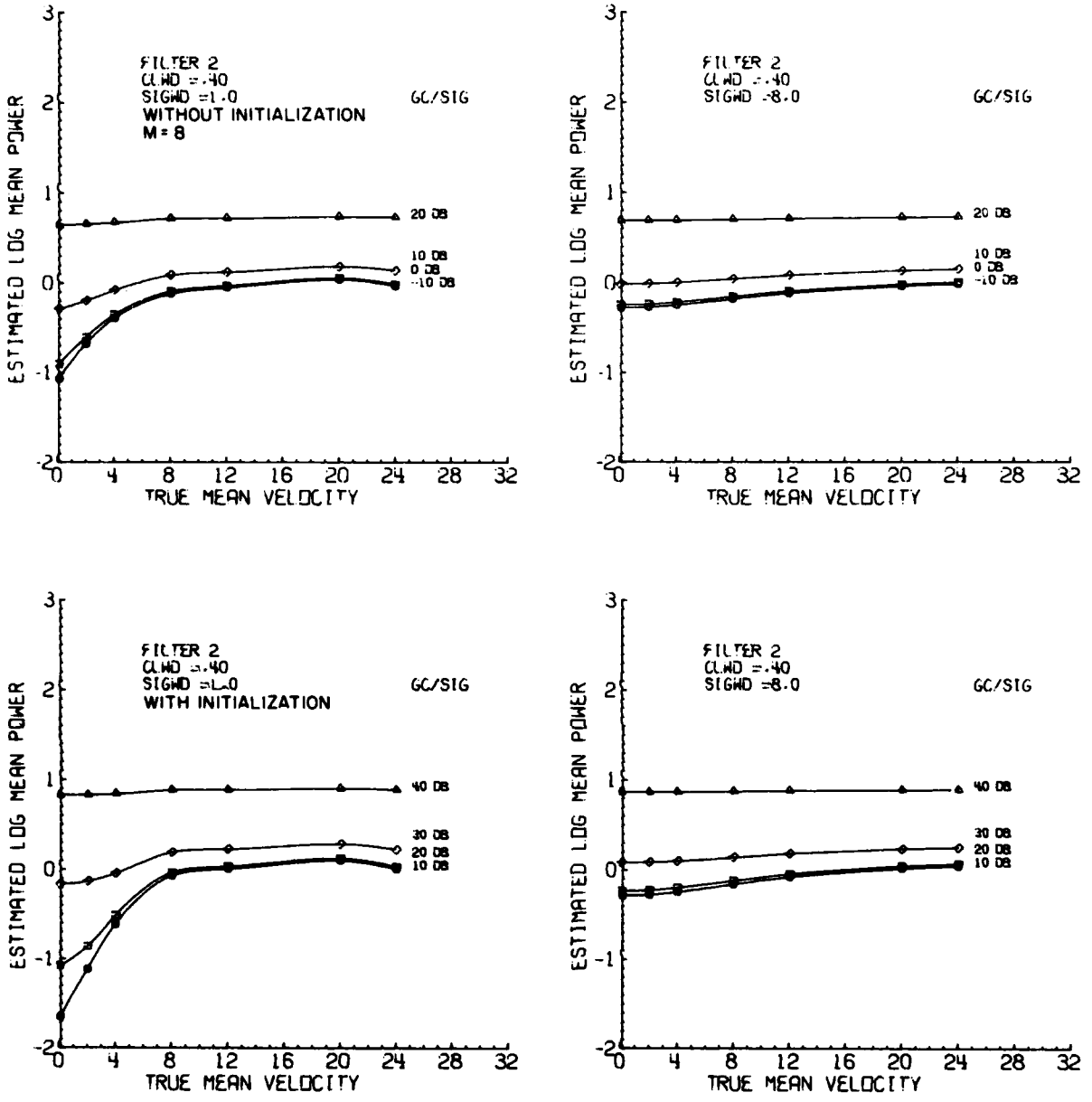

Figure 13. Power estimate after the noninitialized recursive filter (upper graphs) and initialized filter (lower graphs). On the ordinates are logarithms of $P/\overline{P}$ where $\overline{P}$ is the true mean power. Clutter width CLWD is 0.4 $m \cdot s^{-1}$, signal widths SIGWD are 1 $m \cdot s^{-1}$ (on the left), and 8 $m \cdot s^{-1}$ (on the right), and clutter-to-signal power ratio GC/SIG is indicated. Eight samples were passed through the filter, but only the last seven were used for power estimation.

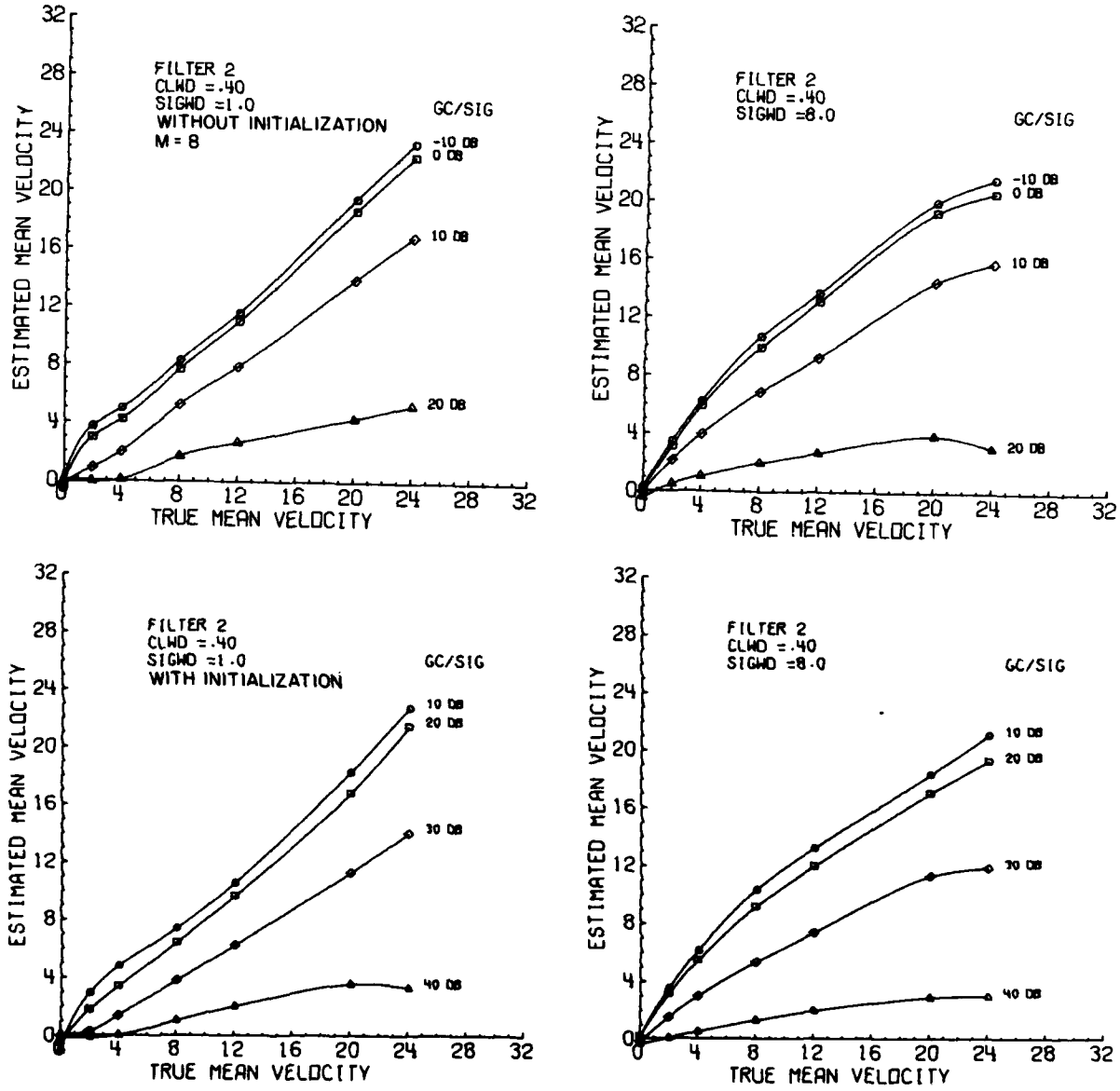

Figure 14. Estimated mean velocity versus true mean velocity for simulated times series data processed by the pulse pair processor. Other parameters are as on Figure 13.

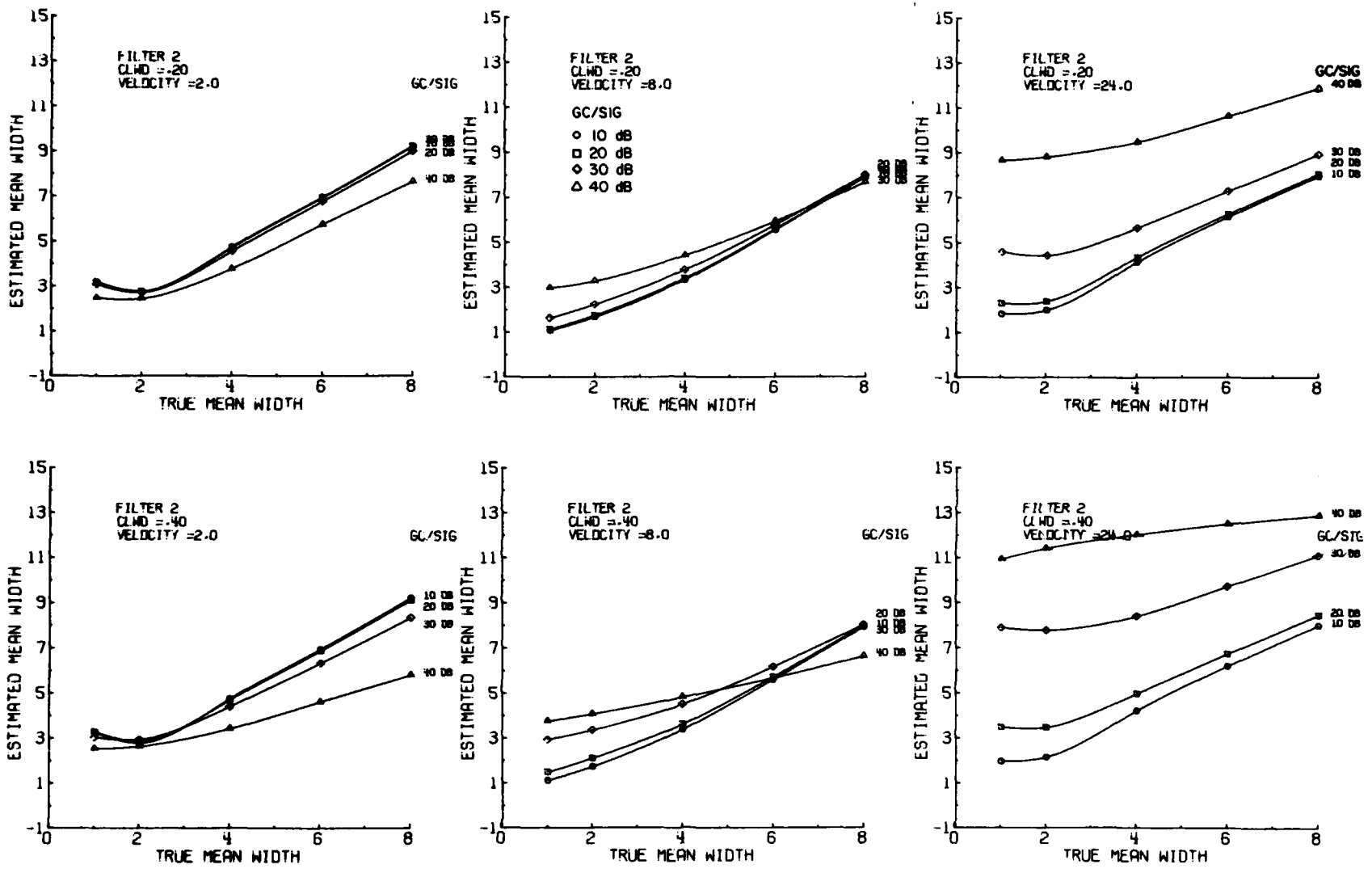

Figure 15. Estimated mean signal spectrum width versus true width for simulated time series data. Thirty-two samples were filtered through the initialized filter but only the last sixteen were applied to the pulse pair processor. Clutter widths are 0.2 $m \cdot s^{-1}$ (upper graphs) and 0.4 $m \cdot s^{-1}$ (lower graphs). The mean signal velocities from left to right are 2, 8, and 24 $m \cdot s^{-1}$.

than 1 $m \cdot s^{-1}$) for clutter-to-signal ratios of 10 and 20 dB, but fall apart at 30 dB and mean velocities larger than 12 $m \cdot s^{-1}$.

5. Design Consideration

The representation of filter coefficients and the architecture of the third order recursive filter are briefly discussed in this section.

Filter coefficients and data in our implementation will be converted to fixed-point fractional numbers. Figure 16 shows the response of the filter with coefficients represented as fixed-point numbers with 10-bit fractional parts, along with the response of the actual filter. As can be seen, the filter performance is quite poor since only 30 dB of cancellation is achieved. The performance at wider stopbands is somewhat better. Figure 17 shows the response of a filter with 12 bits in fractional part, which meets the design objectives.

Figure 18 is the block diagram of the proposed hardware implementation of the three-pole high pass elliptic filter used for ground clutter cancellation. The hardware is based on a high-speed parallel arithmetic and logic unit assisted by four multipliers capable of simultaneous operation. The hardware is capable of performing the entire filtering arithmetic within 1 microsecond, resulting in real-time operation. System control is implemented in microcode to maintain flexibility and facilitate future modifications if required. The control logic operates at a clock rate of 10 MHz. Filter coefficients and constants are implemented in switches, and the filtering range can also be selected by switches. Filter initialization is provided in hardware and is automatically performed when the radar is operating in the expanded (interlaced PRF) mode.

The hardware is implemented with a 16-bit parallel internal data bus. Data and coefficients are represented by fixed-point binary numbers with 12-bit fractional part.

The design and fabrication of the filter are being supported by Joint Systems Program Office, and we anticipate that the device will be operational in the first half of 1983.

6. Conclusions

Problems associated with the first trip clutter overlaying second trip area for velocity and spectrum width estimation have been pointed out. The obscured area in the second trip is larger (by about 10 times for the NSSL radar) than the first trip clutter area. Moreover, the weather signals in the second trip area suffer a range square disadvantage which for the NSSL radar is about 10 to 25 dB. The very important aspect concerning range de-aliasing of velocity estimates has

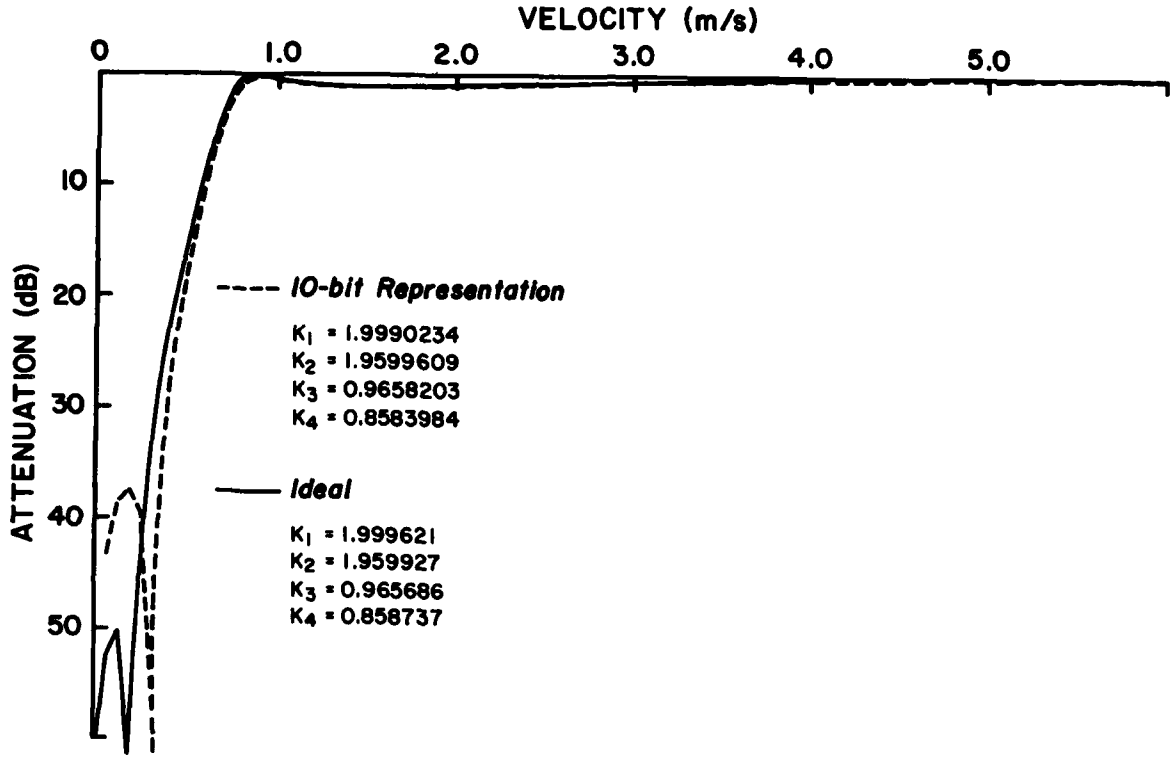

Figure 16. Frequency (velocity) response of a narrow notch filter. Solid line is for ideal coefficients and dashed line is with a 10-bit representation.

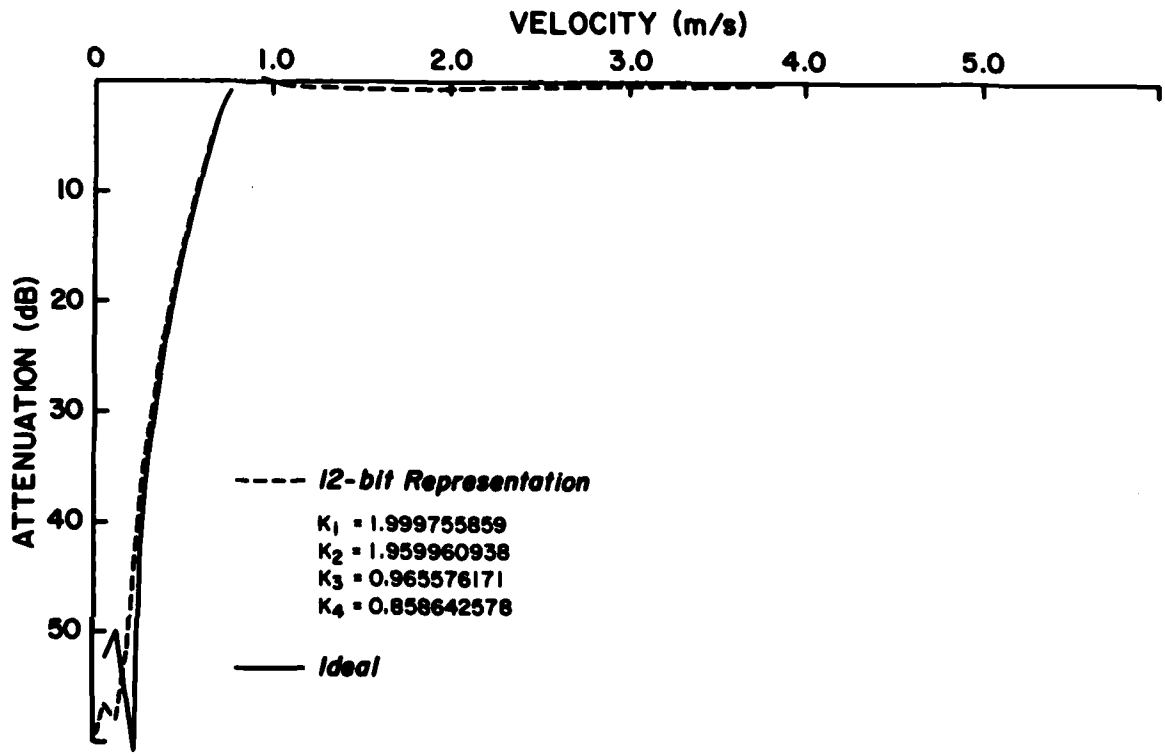

Figure 17. Frequency response of the filter on Figure 16 except a 12-bit representation is used.

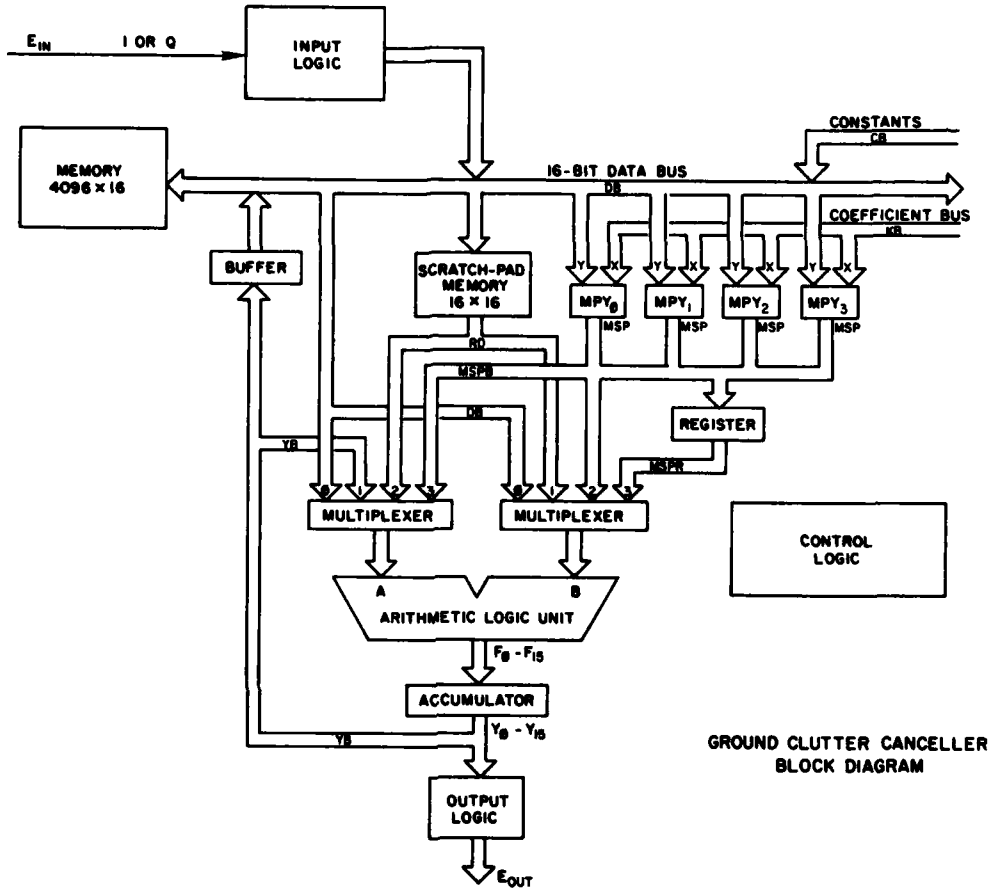

Figure 18. Block diagram of a ground clutter canceler. Coefficients are programmable and the filter can be of order up to three.

been examined. Much work remains to be done in this area to realize the full benefit of the ground clutter canceler in the velocity channel. The optimum, but expensive, solution calls for a dual frequency radar with two coherent receivers and ground clutter filter with almost equal characteristics. Then the powers in the reflectivity channel can be used to assign correct ranges for the velocity estimates. But, with interlaced sampling, clutter filters in the reflectivity and velocity channel would have quite different characteristics; the notch depth would be probably 20 dB deeper in the velocity channel because the dwell time for velocity estimation is longer. Consequently, when powers in the reflectivity channel are compared for assigning correct ranges to the velocities, the full potential of the clutter filter in the velocity channel will not materialize, i.e., some second trip velocities would be falsely declared invalid. A more complicated processing requires comparisons of powers in the reflectivity channel with those in the velocity channel.

The most economical canceling scheme is with a third order recursive filter. This filter achieves a 50 dB rejection in the stopband with total annihilation of DC. One dB ripple is in the passband, and the ratio of passband cutoff v_p to stopband cutoff v_s is about 3.6. The filter operates best in steady state, but it can also be made to operate in transient by properly initializing its memory elements. Performance on 8 simulated time samples shows that about 10 dB of clutter-to-signal margin is lost for power and 20 dB for mean velocity estimation. But with such a small number of samples the width estimate is useless. Thus, interlaced sampling can be used for velocity estimation at a 20 dB penalty in clutter canceling, but it is not suitable for spectrum width estimation.

In order for spectrum width biases to be less than 1 $m \cdot s^{-1}$, a longer train of pulses must be employed on an initialized filter and several of the leading pulses must be used exclusively to further reduce the transients. Then from the rest of the pulses the widths will be credible. Theoretical curves of the expected attenuation for the initialized filter in transient are presented. From these one can determine the number of recursions needed to reduce clutter power below a desired level and thus the number of samples that should not be applied to the pulse pair processor. An example shows that if the first 16 samples out of 32 are solely used to further reduce the transients, spectrum width can be estimated with little bias as long as clutter-to-signal ratio is less than 20 dB.

The part of weather signal that is within the stopband cutoff of the filter is totally lost, but that is a small penalty because zero radial velocities occupy a small portion of a storm and should not affect significantly total areal

rainfall rate estimates. Furthermore, in these instances the mean velocities will be noisy but not biased. However, large spectrum widths indicative of turbulence and other hazards would still be measurable. Therefore, canceling should be done selectively at those ranges and elevation angles where ground clutter is significant.

Examination of hardware for implementing the filter resulted in a preliminary design based on a high speed parallel arithmetic and logic unit assisted by four multipliers capable of simultaneous operation. Two identical units are needed, one for the inphase, the other for the quadrature component of the video signal. The proposed architecture has a throughput rate faster than 1 μs and is thus capable of real time operations.

We stress that clutter canceling is easiest with an uninterrupted pulse train because the recursive filter is then less subject to transients.

7. Acknowledgments

The authors are indebted to Bill Bumgarner for computer support and development of many routines used in this study. Joan Kimpel produced the art work and Joy Walton typed the manuscript.

8. References

Doviak, R. J., D. S. Zrnic', and D. S. Sirmans, 1979: Doppler weather radar. Proc. IEEE, 67, 1522-1553.

Fletcher, H. R., and D. Burlarge, 1972: An initialization technique for improved MTI performance in phased array radars. Proc. IEEE, 60, 1551-1552.

Groginsky, H. L., and K. Glover, 1980: Weather radar canceler design. Preprints, 19th Conf. on Radar Meteor., Apr., Am. Meteor. Soc., Boston, Mass., 192-201.

Hennington, L., 1981: Reducing the effects of Doppler radar ambiguities. J. Appl. Meteor., 20, December, 1543-1546.

Zrnic', D. S., 1975: Simulation of weatherlike Doppler spectra and signals. J. Appl. Meteor., 14, 619-620.

_____, 1979a: Spectrum width estimates for weather echoes. IEEE Trans. on Aerospace and Elec. Syst., AES-1[illegible], 613-619.

_____, 1979b: Estimation of spectral moments for weather echoes. IEEE Trans. on Geosci. Elec., GE-17, 113-128.

Zrnic', D. S., and S. Hamidi, 1981: Considerations for the design of ground clutter cancelers for weather radar. Interim Report April 80 - Feb. 81, IAA DTFA01-80-Y-10524.

END

FILMED

2-83

DTIC